



---

---

## **PREDICTABLE IONOSPHERIC PARAMETERS AND METHODS OF CALCULATING CIRCUIT PARAMETERS FROM PATH GEOMETRY**

**(AN OVERVIEW)**

**BY**

**MOLUA O.C, NWACHUKU, D.N. & EGHENEJI, A.A.**

**PHYSICS DEPARTMENT, COLLEGE OF EDUCATION**

**AGBOR.**

---

---

### **ABSTRACT**

*The presence of free electrons in the ionosphere produces the reflecting regions important to high frequency (HF) radio-wave propagation. This paper presents an overview of predictable ionospheric parameters because at HF, all the regions are important and should be considered in predicting the operational parameters of radio communication circuits. Also presented are propagation by way of sporadic E and other anomalous ionization together with ways of calculating circuit parameters such as path length and bearings as well as the sun's Zenith angle.*

---

---

## INTRODUCTION

### PREDICTABLE IONOSPHERIC PARAMETERS

The presence of free electrons in the ionosphere produces the reflecting regions important to High Frequency (HF) radio-wave propagation. In the principal regions, between the approximate heights of 75 km and 500 km, the electrons are produced by the ionizing effect of ultraviolet light and soft x-rays from the sun. For convenience in studies of radio-wave propagation, the ionosphere is divided into three regions defined according to height and ion distribution: the D,E, and F regions. Each region is subdivided into layers called the D,E, Es, F1, and F2 layers, also according to height and ion distribution. The layer do not show much difference but vary in thickness. At high frequency, the regions show considerable imperatives in predicting the operational parameters of radio communication circuits.

### THE D REGION

The D region is approximately between 75 and 90 km above the earth's surface. There is heavy energy loss due to collision of molecules and free electrons predominant in the D region. When there is optimal bending of the wave, reflection also occurs in the E and F layers. Therefore, for absorption to take place additional time is needed for collisions thus leading to what is normally referred to as retardation effect. In the D-layer ionization is produced by ultraviolet radiation and this occurs at all frequencies.

MOLUA O.C, NWACHUKU, D.N. & EGHENEJI, A.A.

---

---

The degree of absorption in this region is directly proportional to the electron density and collision frequency and also inversely proportional to the square of the frequency.

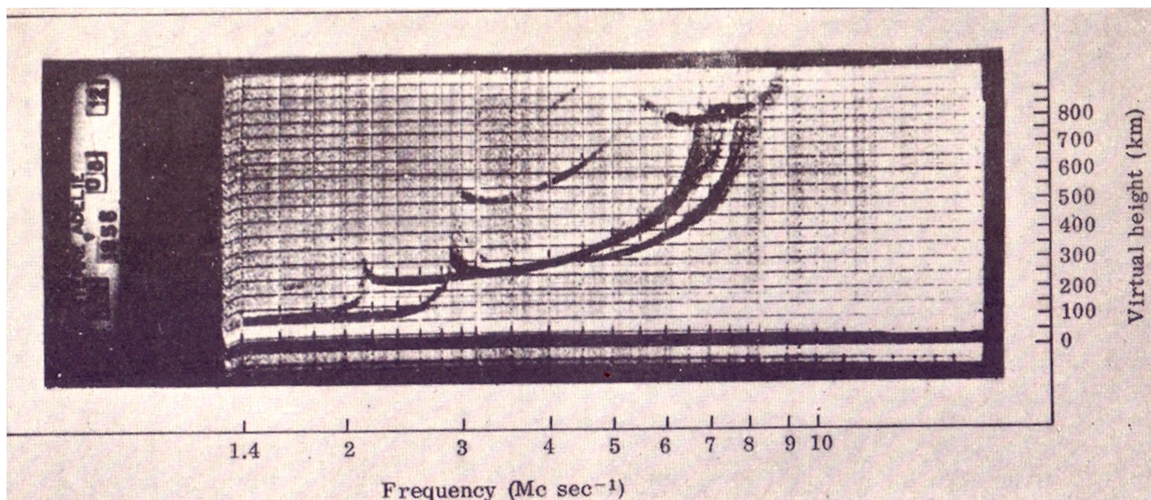
The critical frequency varies with  $\cos x$ - the ionization angle of the sun with this one can determine if a layer is Chapman or not D,E and due to maximum production of electron there.

### THE E REGION

There is little information about the E region of the ionosphere because at night the critical frequency  $f_oE$  lies outside the working range of most ionosonde (Robert G.F. et al 1963)

### MEASUREMENTS

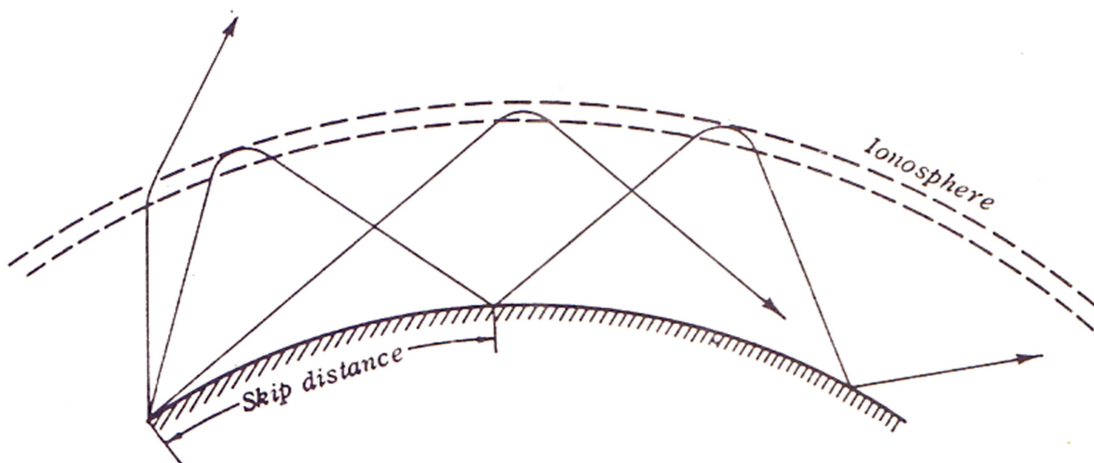
The Phenomenon of Sporadic E is still attracting scholars attention in this region



A typical record on which distinct layers are evident is as shown above.

MOLUA O.C, NWACHUKU, D.N. &amp; EGHENEJI, A.A.

Some sixty ionospheric monitoring stations distributed over the world keep continuous watch on the ion distribution in the atmosphere. In addition to providing the data needed for the description of the ionosphere, which is essential for the maintenance of radio communication, these observations have made possible complex calculations of temperature of composition of the air and of properties of the earth's magnetic field communication over great distances is possible because reflection from the ionosphere can be utilized as shown below.



At a small angle of incidence the beams of radio energy may penetrate the ionosphere, whereas at a larger angle they are reflected. Thus communication is possible far beyond line of sight, but there may be a "skip distance" within which signals cannot be received. Multiple reflections between conducting earth and the ionosphere may make

MOLUA O.C, NWACHUKU, D.N. & EGHENEJI, A.A.

---

---

possible communication half-way or even all the way around the earth optimum frequency is chosen for the relevant distance and ionospheric conditions, and if ion concentration changes in response to change in the ultra –violet emission from the sun, communication may be interrupted until the frequency of the transmitter is changed to a new optimum value. The E-region characteristics that have been systematically scaled from the vertical-incidence ionosonde records include:

- |      |   |
|------|---|
| foE  | The critical frequency of the ordinary component of the E layer; i.e., that frequency at which the signal from the ionosonde just penetrates the E layer. |
| h'E  | The minimum virtual height of the E layer, measured at the point where the trace becomes horizontal.  |
| foEs | The highest observed frequency of the ordinary component of sporadic-E (Es) amongst others.   |

## PREDICTIONS

The regular E layer is predicted using three parameters: the monthly median value of critical frequency (foE), height of maximum ionization of the layer (hmE), and ratio of hmE to semi-thickness (ymE). In the past, the E-layer critical frequency has been determined by a semi-empirical equation involving the sunspot number and the zenith angle of the sun.

MOLUA O.C, NWACHUKU, D.N. & EGHENEJI, A.A.

---

---

Obviously, such a relationship would be inadequate to estimate foE values at sunrise or sunset and during nighttime. Worldwide numerical coefficients of monthly median foE are available for computer applications in terms of geographic latitude, longitude, and universal time. The numerical coefficients (Piddington, 1951) representing foE were derived from measurements taken during 1958 and 1964. These years were selected for analysis because the data are representative of the high (1958) and low (1964) phases of the sunspot cycle. Linear interpolation is used between the representative data for the high (SSN = 150) and low (SSN = 10) sunspot periods to obtain foE estimates at all other phases of the solar cycle.

Little information is available concerning the statistical distribution of the monthly median foE. In daytime, the E layer is sufficiently regular that the distribution spread of the monthly median foE may be considered negligible. Nighttime data are insufficient, but it appears justified (Lyon 1964) to assume a similar regularity for the foE monthly median of the nighttime E layer.

Therefore, we believe that the E-layer characteristics most important for communication purposes are adequately represented by the available foE monthly median numerical coefficients. The approximate true height range of the regular E layer is well established at 90 to 130 km and it is assumed that the maximum electron density occurs at 110 km and the semi-thickness is 20 km (Richards, 2001). With the above assumption, the ratio of the height to the semi-thickness ( $h_m E / y_m E$ ) is assumed to be 5.5.

## THE F REGION

The vertical-incidence ionosonde network with its long series of measurements over much of the world, provides the basis for F-region predictions (Martyn, 1953). The following parameters have been systematically scaled from the vertical ionosonde records (Piggott and Rawer, 1961), although some stations do not report all of them:

- |           |  |
|-----------|--|
| foF2      | The critical frequency of the ordinary component of the F2 layer; i.e., that frequency at which the signal from the ionosonde just penetrates the F2 layer.  |
| M(3000)F2 | The factor for converting vertical-incidence critical frequencies to oblique incidence for a distance of 3000 km via the F2 layer.   |
| foF1      | The critical frequency of the ordinary component of the F1 layer; i.e., that frequency at which the signal from the ionosonde just penetrates the F1 layer.  |
| H'F2      | The minimum virtual height of the F layer; i.e., the minimum virtual height of the night F layer and the day F1 layer. It is measured at the point where the F trace becomes horizontal. (In earlier years the minimum virtual height of the night F layer was often combined with that of the day F2 layer, the combined tabulation being designated h'F2. In |

MOLUA O.C, NWACHUKU, D.N. & EGHENEJI, A.A.

---

---

these cases, the minimum virtual height of the F1 layer,  $h'F1$ , was tabulated separately.)

$h_pF2$  The virtual height of the F2 layer corresponding to a frequency  $f$ , where  $f = 0.834 f_oF2$ . This is based on the assumption of a parabolic ionization distribution, which is usually considered justified as an approximation to the height of maximum ionization of the F2 layer.

For HF radio communications, the F region is the most important part of the ionosphere. It is not regular and because of its variability, short time scale estimates of the important F-region characteristics are required if predictions of the operational parameters of HF radio systems are to be meaningful.

The F1 layer has not been as well defined as the F2 layer in terms of its predictable characteristic features. The F1 layer is of importance to communication only during daylight hours or during ionospheric storms (Bilitza et al, 2004); it lies in the height range of about 200 to 250 km and undergoes both seasonal and solar cycle variations, which are more pronounced during the summer and in high sunspot periods.

## PREDICTIONS

The F2 layer is described by three parameters: monthly median value of critical frequency ( $f_oF2$ ), height of maximum ionization ( $h_mF2$ ), and a ratio of  $h_mF2$  to semi-thickness ( $y_mF2$ ). Monthly median values of  $f_oF2$  and the  $M(3000)F2$  for two solar activity levels are



available as numerical coefficients in terms of a modified magnetic-dip angle and longitude, and universal time (Rishbeth and Mendillo, 2001).

There is also available a more recent model of the F2 region of the ionosphere. This model is based on a combination of observed and theoretical data. The theoretical data provided stability in large regions where no observed data existed, such as ocean areas and non-industrialized areas. (Sardar et al, 2012) This F2 region model showed minor improvements in populated regions and significant improvements over sea area and unpopulated regions when compared to observed ionosound and satellite measurements. The analytical structure of the more recent coefficients and the documentation would be consistent. The solar activity dependence is accounted for by linear interpolation.

## **PROPAGATION BY WAY OF SPORADIC E AND OTHER ANOMALOUS IONIZATION**

In the preceding discussion of the important regions of the ionosphere, we concentrated on the first order characteristics of the various layers. There are many other characteristic phenomena, e.g., sporadic E, spread F, F scatter, multiple traces, and other transients, often observed on ionosonde records (Piggott and Rawer, 1961), that are important in radio communications; however, present prediction schemes demand that the general ionospheric structure be statistically representative and in a continuous sequence. Of these phenomena, the only one we have been able to partly represent for prediction purposes is the sporadic-E layer.

## SPORADIC E

Sporadic E (Matsushita, 1959) is seen on vertical and oblique ionograms near the height of maximum ionization of the regular E layer. Sporadic E(Es) is characterized by little or no retardation at its critical frequency and may be either blanketing (totally reflecting) or semitransparent (partly reflecting), or both, up to very high frequencies( >75 MHz). These characteristics can be helpful or harmful to radio communications. For example, blanketing Es may block propagation via a more favorable regular layer mode in a certain frequency range or cause additional attenuation at other frequencies. Partially reflecting Es can cause serious multipath and mode interference, especially detrimental to data transmission systems. However, Es may extend the useful frequency range and its presence can be effectively used in system design and operations.

The physical processes that produce sporadic-E ionization are not fully known, but it is generally accepted that the mechanisms may be quite different in auroral, temperate, and equatorial geographic areas (Ractliffe, 1956). In auroral areas, energetic particles appear to play a vital role in the production of sporadic E (Zhang et al, 2008). Temperate-area Es is best explained by the behavior of upper atmosphere winds (Matsushita 1959) and a related wind-shear theory (Bilitza, 2001). In equatorial areas, i.e., in a narrow  $\pm 6^\circ$  belt centered on the magnetic dip equator, the production of sporadic-E is explained by theories on plasma instability phenomena (Basu et al 2002).

MOLUA O.C, NWACHUKU, D.N. & EGHENEJI, A.A.

---

---

Methods of forecasting sporadic E are influenced by the physical processes involved and should be considered in all prediction schemes. In this report, we are not directly concerned with forecasting techniques, but with predicting operational parameters when sporadic E is the dominant propagation mode. Therefore, the numerical coefficients representing the monthly statistical distribution of foEs for any location are empirically derived estimates of sporadic E during periods of solar cycle minimum and maximum, and they are used only when propagation via the regular E layer is not possible.

It may be helpful to review the general occurrence characteristics of sporadic E for the three geographic areas mentioned above (Bilitza, 2001):

Auroral Es - Occurs mainly at night at geomagnetic latitudes greater than about  $60^\circ$ , with a maximum near  $69^\circ$ . Its seasonal, diurnal, and solar cycle patterns are not clear. It occurs more frequently during periods of high magnetic activity and follows the sudden commencement associated with a solar flare (Bates, 1960).

Temperate Es - Characterized by a pronounced maximum during the summer solstices (June-July in the Northern Hemisphere and December-January in the Southern Hemisphere). A seasonal minimum occurs during the vernal equinox; this minimum changes abruptly at  $60^\circ$  geomagnetic latitude. The diurnal pattern exhibits peaks during mid-morning hours and near sunset. It is primarily observed during the daylight hours and shows a complicated dependence on the sunspot cycle.

MOLUA O.C, NWACHUKU, D.N. & EGHENEJI, A.A.

---

---

Equatorial Es - A regular daytime occurrence without seasonal dependence. It is highly transparent (partly reflecting) and reaches high ( $\approx 50$  MHz) frequencies. Values of foEs around 10 MHz are regularly observed by ionosondes near the geomagnetic dip equator. The reflection properties depend on the direction of propagation; higher reflection coefficients are to be expected for north-south paths.

## PREDICTIONS

Numerical coefficients are available for each month representing the median and decile values of foEs in terms of a modified magnetic-dip angle and longitude, and universal time (Yokoyama and Danilov, 2004). These numerical maps are from data taken during periods of solar activity minimum (1954) and solar activity maximum (1958). Linear interpolation is used for other levels of solar activity. Unless other information is available, the virtual height of the sporadic-E layer is assumed to be 110 km.

## ELECTRON DENSITY PROFILE MODEL

Frequency versus virtual height traces of the ordinary wave as available on vertical incidence ionograms can be converted into electron density profiles by a standard reduction program. These profiles, including geographic, diurnal, seasonal, and solar cycle variations, are generated between heights of 70 km and the height of maximum of the F2 layer, hmF2.

MOLUA O.C, NWACHUKU, D.N. & EGHENEJI, A.A.

---

---

The electron density is given by the relationship

$$N = 1.24 \times 10^{10} f_N^2 \text{ -----} (*)$$

N = electrons per cubic meter

$f_N$  = plasma frequency MHz

The current method of profile generations replaces the parabolic layer structure with a Chapman layer structure. The parabolic layer is analytically more tractable but the Chapman layer has the advantage that a layer whose process is dominated by electromagnetic ionization and chemical losses is closely described by the Chapman layer. In addition, the Chapman layer decreases exponentially with altitude above the layer peak -- this again more closely describes the ionospheric situation. (Mc. Namara and Smith (1982).

## **CALCULATION OF CIRCUIT PARAMETERS FROM PATH GEOMETRY**

To determine the operational parameters for an HF ionospheric radio communication circuit, it is necessary to calculate several parameters that are based on the geometry of the path, such as path length, path bearings, and zenith angle of the sun.

### **PATH LENGTH AND BEARINGS**

The first parameter to be calculated, given the geographic latitude and longitude of the transmitting and receiving locations, is the path length, which is taken to be the shorter of the great-circle distances between the two points, and which is computed as follows:

MOLUA O.C, NWACHUKU, D.N. & EGHENEJI, A.A.

---

$$\cos d = \sin x_1 \sin x_2 + \cos x_1 \cos x_2 \cos(y_1 - y_2), \text{----- (1)}$$

where

$x_1$  = geographic latitude of transmitter,

$y_1$  = geographic longitude of transmitter,

$x_2$  = geographic latitude of receiver,

$y_2$  = geographic longitude of receiver,

$d$  = path length in radians.

Having obtained the path length, we calculate the bearing of transmitter to receiver and receiver to transmitter along the great circle path:

$$\cos b_1 = (\sin x_2 - \sin x_1 \cos d) / (\cos x_1 \sin d) \text{----- (2)}$$

$$\cos b_2 = (\sin x_1 - \sin x_2 \cos d) / (\cos x_2 \sin d) \text{----- (3)}$$

where

$b_1$  = bearing transmitter to receiver in radians,

$b_2$  = bearing receiver to transmitter in radians.

MOLUA O.C, NWACHUKU, D.N. & EGHENEJI, A.A.

---

---

## REFLECTION AREA COORDINATES

In the development of a profile of electron density along the path, the ionospheric parameters at from one to five reflection areas along the path are evaluated depending on the path length. These five areas are:

1. The midpoint of the path.
2. The E-region reflection area nearest the transmitter for the estimated least possible number of hops.
3. The E-region reflection area nearest the receiver for the same number of hops.
4. The F-region reflection area nearest the transmitter for the estimated least possible number of hops.
5. the F-region reflection area nearest the receiver for the same number of hops.

The estimated least possible number of E-layer and F-layer hops is determined from the following relationship to path length:

$$1E, 1F - 0000 \text{ km} \leq \text{path length} < 2000 \text{ km.}$$

$$2E, 1F - 2000 \text{ km} \leq \text{path length} < 4000 \text{ km.}$$

$$4E, 2F - 4000 \text{ km} \leq \text{path length} < 8000 \text{ km.}$$

$$6E, 3F - 8000 \text{ km} \leq \text{path length} < 12,000 \text{ km.}$$

MOLUA O.C, NWACHUKU, D.N. & EGHENEJI, A.A.

For paths less than 2000 km, only the path midpoint is considered. This establishes the reflection areas for determining the ionospheric characteristics for the entire path.

To evaluate the ionospheric parameters of these five reflection areas, their geographic coordinates and geomagnetic latitude have to be computed as follows:

$$x_n = 90^\circ - \arccos(\cos d_n \sin x_1 + \sin d_n \cos x_1 \cos b_1) \text{-----(4)}$$

$$y_n = y_1 - \arccos((\cos d_n - \sin x_n \sin x_1)/(\cos x_n \cos x_1)) \text{-----(5)}$$

$$g_n = 90^\circ - \arccos(\sin 78.5^\circ \sin x_n + \cos 78.5^\circ \cos x_n \cos (y_n - 69.0^\circ)), \text{-----(6)}$$

where

$d_n$  = angular distance of reflection area from transmitter,

$x_n$  = geographic latitude of reflection area,

$y_n$  = geographic longitude of reflection area,

$g_n$  = geomagnetic latitude of reflection area.

The modified magnetic dip latitude is required at each control point for the evaluation of the ionospheric parameters. The magnetic dip can be calculated from the 1963 IRI model of the earth's magnetic field (chou and Lee, 2008) The corrected geomagnetic latitude and longitude is required to define the location and structure of the polar ionosphere.



MOLUA O.C, NWACHUKU, D.N. & EGHENEJI, A.A.

---

---

Computation of the corrected geomagnetic coordinates begins by starting in the equatorial plane at the same point with a dipole field line and a spherical analysis field line, and then calculating the distance between the "landing points" of the two field lines on the earth. In its simplest form, the method consists of labeling the spherical analysis field lines (sometimes called the real field lines) with the coordinates of the coincident equatorial, dipolar field lines. That is, the spherical analysis field has numerous irregularities due to regional anomalies and so it is difficult to assign a meaningful symmetric grid pattern to such a system. However, superimposing the symmetric dipolar grid system on the "realistic" spherical analysis produces a useful coordinate system for modeling purposes.

### SUN'S ZENITH ANGLE

For the first three reflection areas, the zenith angle of the sun is needed for each hour of the day, to be used later in calculating the absorption factor, and is computed from the following equation:

$$\cos \chi = \sin x_n \sin s_x + \cos x_n \cos s_x \cos(s_y - y_n), \text{-----(7)}$$

where

$t_g$  = universal time,

$s_y = 15 t_g - 180$  = subsolar longitude,

$s_x$  = subsolar latitude for the middle of the month,

$\chi$  = sun's zenith angle.

## **TYPES OF PATHS CONSIDERED**

Up to six ray paths are evaluated for each hour and each designated frequency. These ray paths are interpolated from the reflectrix table for the frequency with the distance calculated using a corrected version of Martyn's Theorem for the equivalence of oblique and vertical heights of reflectivity.

## REFERENCE

- Bates, D.R. (1960). Physics of the Upper atmosphere Pp. 378 Academic Press New York
- Bilitza, D, Obrou, O.K., Adeniyi, J.O, Oladipo, O. (2004) Variability of foF<sub>2</sub> in the equatorial ionosphere Advances in Space Research 34, 1901-1906.
- Budden, K.G (1966) replaces Berghansen, 1966 Radio waves in the ionosphere. Cambridge University press (pg. 2) Cambridge.
- Chou, Y.T, and Lee C.C. (2008) Ionospheric Variability at Taiwa Low latitude Station: Comparison between observations and IRI- 2001 model, Adv. Space Res. 673-681
- Friedman, H. (1963): Ionospheric constitution and ionizing radiation in the ionosphere Inst. Phy. And Phys. Society London.
- Kelso, J.M (1954): The Determination of Electron Density Distribution J. Atoms. Terr. Phy. 10, 103-109
- Lyon, E.O (1964): Noon time variation of foE with relative sunspot number, RZ. Journal Afr. Earth Science 5. 193.
- Martyn, D.F (1953): The Morphology of the ionospheric Variations Associated with magnetic disturbance Proc. Roy. Society. London A 218, 1-18
- Matsushita, S. (1959). A study of the Morphology of ionospheric Storms. J. Geophys. Res. 64, No. 3, 305-321
- Mc Namara. L.F. and Smith, D.H. (1982). Total electron content of the ionosphere at 3105, 1967-1974. J. Atoms. Terr. Phy. 44, 227-239
- Piddington J.H (1951): The modes of formation of the ionospheric layers. J. Geophys. Res. 56 No. 3. 409-429
- Ractliffe, J.A (1956): A quick method for analyzing ionospheric records. J. Geophys. Res. 56 No. 463-485

**MOLUA O.C, NWACHUKU, D.N. & EGHENEJI, A.A.**

---

---

Robert G. F. et al (1963): An Introduction to Atmospheric Physics. Academic Press New York

U.R.S.I. Hand book of Ionogram interpretation and Reduction by Piggot W.R and Rawer, K.  
Elsevier Publishing Co. 1961)

Yokoyama, T and Davilov A.D (2004) Relationship of the onset of the Equatorial E-region  
irregularities with the sun-set terminator observed with the equatorial atmosphere.  
Radar. Geophy. Res. Lett. 31. L24804